

# Coulomb broadening of nonlinear resonances in optical spectra of ions

S. A. Babin, V. I. Donin, and D. A. Shapiro

*Institute of Automation and Electronics, Siberian Division, USSR Academy of Sciences*

(Submitted 31 March 1986)

Zh. Eksp. Teor. Fiz. **91**, 1270–1279 (October 1986)

A theory is developed of the broadening of nonlinear resonances in an ion-laser plasma via Coulomb diffusion of ions in velocity space in the field of a strong light wave. It is shown that the Coulomb and field broadenings add up linearly. The dependences of the width of the Lamb dip in an argon laser on the density of the charged particles were measured for the first time for lasing lines at wavelengths 4880 and 5017 Å. It is established that the dip broadening is of Coulomb origin.

## §1. INTRODUCTION

Broadening of nonlinear spectral resonances in a gas has been the subject of many studies (see, e.g., Refs. 1 and 2 and the bibliography therein). In practically all the studies, however, the pair-collision approximation was used. This approach is valid if the effective radius of the atom interaction is less than the average distance between the atoms. This condition is met, in particular, by active media of neutral-atom lasers. The plasma of coherently emitting ionized-gas lasers contains interacting charged particles whose scattering by one another is essentially of the many-particle type because of the slow decrease of the Coulomb forces with distance. The influence of Coulomb scattering on the forms of spectral resonances is therefore of particular interest for both nonlinear spectroscopy and ion-laser physics.

Spectral-line broadening via Coulomb interaction was first investigated theoretically in Ref. 3, where it was shown that the broadening is caused by the action of the electric-field fluctuations in the plasma on the translational motion of the ion. The calculation was carried out by perturbation theory in terms of the strength of the optical field. An approximate estimate of the role of the effect under argon-laser plasma conditions is given in Ref. 4, but only an order-of-magnitude comparison with experiment was obtained, since the separation of the Coulomb broadening from the field broadening was not considered. Note that the relatively large broadening of the Lamb dip in ion lasers has not yet been exhaustively explained to date on the basis of the known broadening mechanisms (see the reviews by Davis and King<sup>5</sup> and by Dunn and Ross<sup>6</sup>). This is due for the most part to the absence of detailed experimental investigations, particularly simultaneous measurements of the homogeneous width and of the charged-particle density.

Our aim was to determine experimentally the Lamb-dip broadening in an argon laser as a function of the charged particle density, to generalize the Coulomb-broadening theory to include the case of strong light fields, and to compare quantitatively the experimental data with the theory. In §2 is given the theory of nonlinear-resonance broadening in a strong light field. The measurement procedure and results are the subject of §3. The dependences of the total width of the Lamb dip on the plasma parameters were measured for

two ArII laser lines with wavelengths 4880 Å ( $4s^2P_{3/2} - 4p^2D_{5/2}^0$ ) and 5017 Å ( $3d^2D_{3/2} - 4p^2F_{5/2}^0$ ).

The 5017 Å line is preferred for the study of broadening because of its relatively small natural width (295 MHz), as against a radiative width  $\sim 460$  MHz for other ArII lasing lines.<sup>5-7</sup> The theory and experiment are compared in §4, where alternate broadening mechanisms and other possible sources of systematic errors are analyzed. From the quantitative agreement between the theory and the measurement results, conclusions are drawn in §5 concerning the nature of the observed broadening.

## §2. COULOMB BROADENING IN A STRONG LIGHT FIELD

It is known that broadening of nonlinear resonances can be described on the basis of the quantum kinetic equation for the Wigner density matrix  $\rho_{ij}(\mathbf{r}, \mathbf{v}, t)$  (see Ref. 1):

$$\left(\frac{\partial}{\partial t} + \mathbf{v} \nabla_{\mathbf{r}} + \gamma_{ij}\right) \rho_{ij} = S_{ij} + q_j \delta_{ij} + i[V, \rho]_{ij}, \quad l, j = m, n. \quad (2.1)$$

Coulomb interaction of resonant ions with other charged particles, and also relaxation processes that can be taken into account in the impact approximation, are described by the collision term  $S_{ij}$ . We denote by  $\gamma_{ij}$  the radiative-decay constants and by  $q_j$  the rates of excitation of the states  $j$ . Resonant interaction of the ions with the field represented by a standing wave is accounted for by the operator  $V$  with matrix elements

$$V_{mn} = G e^{-i\alpha t} \cos \mathbf{k} \mathbf{r}, \quad G = \mathbf{E} \mathbf{d}_{mn} / 2\hbar, \quad \Omega = \omega - \omega_{mn}, \quad (2.2)$$

where  $\mathbf{E}$  is the amplitude,  $\omega$  the field frequency,  $\mathbf{d}_{mn}$  the electric dipole moment, and  $\omega_{mn}$  the Bohr frequency of the  $m$ - $n$  transition.

That part of the collision integral which describes the Coulomb diffusion in velocity space is described in terms of the particle-flux vector<sup>3</sup>

$$S'_{ij} = \frac{\partial}{\partial v_{\alpha}} \int \frac{d\mathbf{v}'}{m} U_{\alpha\beta}(\mathbf{v}, \mathbf{v}') \left( \frac{\partial f'}{\partial v_{\beta}'} \frac{\rho_{ij}}{m'} - \frac{f'}{m} \frac{\partial \rho_{ij}}{\partial v_{\beta}} \right), \quad (2.3)$$

$\alpha, \beta = x, y, z$ ;  $f' = f'(\mathbf{v}')$  is the distribution function of the perturbing particles,  $m'$  their mass, and  $m$  the mass of the resonant ion. The kernel of the Landau collision integral<sup>8</sup> takes the form

$$U_{\alpha\beta}(v, v') = 2\pi L e^4 Z^2 Z'^2 (u^2 \delta_{\alpha\beta} - u_\alpha u_\beta) / u^3, \quad (2.4)$$

where  $L$  is the Coulomb logarithm,  $\mathbf{u} = \mathbf{v} - \mathbf{v}'$  is the relative velocity of the particles, and  $Z$  and  $Z'$  are their charges in units of the electron charge  $e$ . Summation over repeated indices, and if necessary also over the species of the perturbing particles, is implied in (2.3). Other types of broadening are taken into account in the relaxation-constant model. The Landau kernel is obtained from the Boltzmann collision integral in which only small-angle scattering events are retained and the integral over the impact parameters is cut off at the Debye screening radius. Ion interaction via collective plasma oscillations is described by a Landau-integral addition that is significant only in a strongly nonisothermal plasma.<sup>9</sup>

If the level-excitation functions and the perturbing-ion velocity distribution functions are Maxwellian, viz.,

$$f'_i = n_i W(v'), \quad q_j = Q_j W(v), \quad W = (\sqrt{\pi} v_{Ti})^{-3} \exp(-v^2/v_{Ti}^2), \quad (2.5)$$

an explicit expression can be obtained for the dynamic-friction force and for the diffusion tensor in velocity space. If furthermore the effective frequency  $\mu$  of the Coulomb ion-ion collisions is low enough,  $\mu/\Gamma_j < \Gamma_{mn}/kv_{Ti} \ll 1$ , where  $\Gamma_j$  is the relaxation constant of the  $j$ th level and  $\Gamma_{mn}$  and  $kv_{Ti}$  are respectively the homogeneous and Doppler line widths, dynamic friction can be neglected compared with diffusion.<sup>10</sup> At  $v < v_{Ti}$  the calculations can be simplified by using also the smallness of the off-diagonal components of the diffusion tensor and assuming the diagonal ones to be independent of velocity. The collision integral (2.3) reduces then to a simple differential operator

$$S_{ij}' = D \Delta_v \rho_{ij}, \quad D = \mu \frac{v_{Ti}^2}{2}, \quad \mu = \frac{16\pi^{3/2} n_i L (e^2 Z Z')^2}{3m^2 v_{Ti}^3}, \quad (2.6)$$

that describes Brownian motion. The influence of such collisions in a strong optical field on the Doppler contour of the spectral line was investigated in Ref. 11. We are interested in the profile of the narrow nonlinear resonance.

The lower level in the active medium of an ionized-gas laser usually decays rapidly  $\Gamma_m \ll \Gamma_{mn}, \Gamma_n$ . We use this condition to calculate the Bennett-hole contour in the upper-level population distribution in the component  $v_{\parallel}$  of the velocity  $\mathbf{v}$  along the wave vector  $\mathbf{k}$ . In the spectroscopic limit  $\Gamma_{mn} \ll kv_{Ti}$  we can neglect also the transverse part of the Laplace operator. For the stationary population  $\delta_m$  in a traveling-wave field we obtain a one-dimensional Schrödinger equation with a source and potential in Lorentzian form:

$$-D \frac{d^2 \rho_m}{dv_{\parallel}^2} + \left( \Gamma_m + \frac{2|G|^2 \Gamma_{mn}}{\Gamma_{mn}^2 + (\Omega - kv_{\parallel})^2} \right) \rho_m = q_m. \quad (2.7)$$

The coefficients of (2.7) have two regular points  $v_{\parallel} = (\Omega \pm i\Gamma_{mn})/k$  and one essential singularity  $v_{\parallel} = \infty$ . Transforming to nondimensional variables and replacing the unknown function

$$\begin{aligned} \varepsilon &= \frac{Dk^2}{\Gamma_{mn}^2 \Gamma_m} & \kappa &= \frac{2|G|^2}{\Gamma_{mn} \Gamma_m}, \\ x &= \frac{\Omega - k\mathbf{v}}{\Gamma_{mn}}, & \rho_m &= u(x) (1+x^2)^{-1/2}, \end{aligned} \quad (2.8)$$

we can reduce (2.7) to the equation for oblate spheroidal functions (see Refs. 12 and 13). Investigation of these functions is considerably more difficult than that of ordinary special functions, since there are not enough simple integral representations of spheroidal functions. We shall therefore find below an approximate solution of (2.7) in terms of elementary functions.

To this end we formulate the problem for the auxiliary function  $\psi(x) = 1 - \rho_m(x)/\alpha$  as a variational principle

$$S[\psi] = \int_{-\infty}^{\infty} \left[ \varepsilon \left( \frac{d\psi}{dx} \right)^2 + \left( 1 + \frac{\kappa}{1+x^2} \right) \psi^2 - \frac{2\kappa}{1+x^2} \psi \right] dx = \min, \quad (2.9)$$

where  $\alpha = \rho_m(\infty) = q_m/\Gamma_m$ . The unknown function  $\psi$  was chosen because it decreases as  $x \rightarrow \infty$ . One can regard  $\alpha$  as independent of  $x$  if the solution shows that the characteristic width of the function  $\psi$  is significantly less than the large parameter  $kv_{Ti}/\Gamma_{mn}$ . We seek the solution in the form of a Lorentzian

$$\psi = a\gamma / (\gamma^2 + x^2), \quad (2.10)$$

and obtain the parameters  $a$  and  $\gamma$  by minimizing the function  $S(a, \gamma)$ . As a result, the amplitude  $a$  is expressed in terms of the width  $\gamma$ :

$$a = \frac{2\kappa\gamma / (\gamma+1)}{1 + \varepsilon/2\gamma^2 + \kappa(2\gamma+1)/(\gamma+1)^2}, \quad (2.11)$$

for which we obtain in turn the quartic equation

$$\gamma^4 - (1 + \varepsilon/2 + \kappa)\gamma^2 - 2\varepsilon\gamma - 3\varepsilon/2 = 0. \quad (2.12)$$

In the limiting case  $\varepsilon \ll 1$ , when there is no Coulomb broadening, the largest root of Eq. (2.12) is  $\gamma = (1 + \kappa)^{1/2}$ . The known expression for the Bennett hole field broadening is obtained. In the other limiting case of pure Coulomb broadening ( $\kappa \ll 1$ ) a factor  $\gamma + 1$  is separated in (2.12) and the equation becomes cubic. Its solutions for the cases of strong and weak Coulomb broadening are

$$\gamma - 1 = \begin{cases} 2\varepsilon, & \varepsilon \ll 1 \\ (\varepsilon/2)^{1/2}, & \varepsilon \gg 1 \end{cases}. \quad (2.13)$$

To change to the dimensional width we must multiply the last expression by  $\Gamma_{mn}$ . Let us compare (3.13) with the formula proposed in Ref. 10 for the weak-collision model. The coefficients of  $\varepsilon$  and  $\varepsilon^{1/2}$  differ by 50 and 20%, respectively.

Figure 1 shows typical contours of the broadened Bennett hole  $f(x)/\kappa$  obtained by numerically solving Eq. (12.7) with the aid of the run-through algorithm. The error of the approximating Lorentzian (2.10) does not exceed  $2 \cdot 10^{-2} \psi(0)$  and is approximately equal to the width of the line in the figure. The dip broadens when the parameters  $\kappa$  and  $\varepsilon$  are increased.

The level lines of the function  $\gamma(\varepsilon, \kappa)$  are shown in Fig.

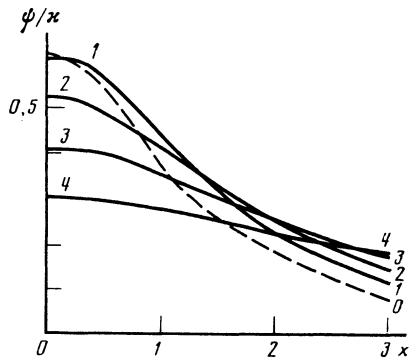


FIG. 1. Contours of field-broadened Bennett hole,  $\kappa = 0.33$ , for various parameters of the Coulomb broadening: 0— $\varepsilon = 0$ ; 1—0.33; 2—1; 3—3; 4—9.

2. It follows from (2.12) that they are straight-line segments. It can be seen from the figure that the Coulomb ( $\varepsilon$ ) and field ( $\kappa$ ) broadenings make nonlinear contributions to the total width. Since the total width is more sensitive to the value of  $\varepsilon$  as  $\kappa \rightarrow 0$ , and the reduction of the experimental data becomes simpler, it is expedient to carry out the measurements at small saturation parameters  $\kappa$ . The result in this case is a simple equation for the Coulomb parameter  $\varepsilon$  as a function of the total width  $\gamma$ :

$$\varepsilon = 2\gamma^2(\gamma - 1) / (\gamma + 3). \quad (2.14)$$

The amplitude of the dip (2.11), which is proportional to the saturation parameter  $\kappa$ , depends quite weakly on  $\varepsilon$  in this case. The ratio  $a/\kappa$  tends to unity both as  $\varepsilon \rightarrow 0$  and as  $\varepsilon \rightarrow \infty$ . The maximum value of this ratio is  $9/8$  and is reached at  $\varepsilon = 6$  ( $\gamma = 3$ ).

The condition for the validity of the foregoing equations is smallness of the homogeneous, Coulomb, and field broadenings compared with the inhomogeneous width of the ion spectral line. Note that at  $\kappa \ll 1$  the contour of the Lamb dip in the frequency dependence of the lasing power has the same shape as the Bennett hole in the population distribution in the longitudinal component of the velocity. The results of the Lamb-dip-profile measurements can therefore be reduced by using Eq. (2.14) after first substituting  $\varepsilon \rightarrow \varepsilon/4$ .

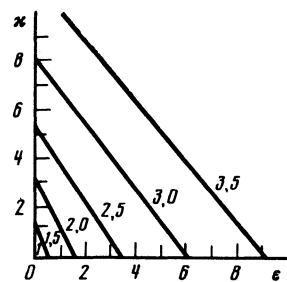


FIG. 2. Level lines of dimensionless width  $\gamma$  of nonlinear resonance vs the parameters  $\varepsilon$  and  $\kappa$ . The numbers on the lines are the values of  $\gamma$ .

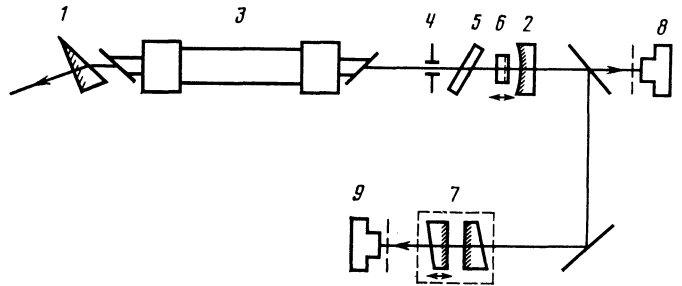


FIG. 3. Diagram of experimental setup: 1—Littrow prism, 2—spherical mirror ( $R = 10$  m), 3—discharge tube, 4—diaphragm, 5—quartz plate, 6—absorbing film, 7—Fabry-Perot interferometer, 8, 9—photoreceivers.

### §3. MEASUREMENT OF THE LAMB-DIP WIDTH IN AN ARGON LASER

The dependence of the lasing power  $P$  on the frequency  $\Omega$  was recorded by the scheme of Fig. 3 in analogy with Refs. 4 and 14. The basis was the laser design described in Ref. 15. The cavity, made up of a Littrow prism 1 and a spherical mirror 2, contained a high-current discharge tube 3 of inside diameter 7 mm and active length 70 cm. Owing to the low gain on the  $5017 \text{ \AA}$  line, mirrors with transparency coefficient not larger than 0.5% were used. Diaphragm 4 of 1.7 mm diameter separated the fundamental transverse mode. Additional losses could be introduced by rotating quartz plate 5.

Frequency selection was with the aid of a thin gold absorbing film<sup>16</sup> with a transmission coefficient 0.69 or 0.75 in the traveling wave. The film was placed near the spherical mirror. The film position in the cavity was scanned by a KP-1 piezoceramic on which an ac voltage of frequency 0.5–10 Hz was applied. The laser emission spectrum was monitored with a Fabry-Perot interferometer of 10 cm base. The dependence of the lasing power  $P$  on the voltage was recorded on the linear section of the characteristic of the piezoceramic. To monitor the possible distortions, several orders of  $P(\Omega)$  in different pass directions were recorded. The resultant contours were identical. The hysteresis of the characteristic shifted the entire pattern without distortion.

A typical  $P(\Omega)$  plot has a noticeable asymmetry. The Lamb-dip asymmetry in gas lasers is usually due to the radial inhomogeneity of the field in the active medium (see Ref. 17 and the literature cited therein). The cavity configuration employed permitted a substantial lowering of this asymmetry.<sup>18</sup> A quasisymmetric contour was observed at saturation-parameter values  $\kappa \approx 0.2$ .

Under the experimental conditions, the lasing line width in the single-frequency regime was usually about 150 MHz, considerably higher than the intermode interval (75 MHz). The frequency fluctuations were due mainly to the noise in the discharge-tube cooling system and to the failure to use special measures to damp the cavity vibrations.

We determined in addition the temperature and drift velocity of the ions by the traditional method of measuring

the Doppler width and the shift of the ion lines (see Ref. 14). The spontaneous-emission line shape was recorded with a Fabry-Perot interferometer having a base 1 cm. The measurements were made for the 4800 and 5145 Å lines, which were separated with an MDR-2 monochromator. In the reduction of the Voigt contour (using the tables), account was taken of the line narrowing due to the gain, as well as of the instrumental width of the interferometer. Under the experimental conditions, the Doppler width  $\Delta\nu_D = kv_{Ti} (\ln 2)^{1/2} \pi$  was 6–9 GHz. The electron density in the same discharge tube was measured the nonlinear dispersion interferometry method proposed in Ref. 19. Depending on the discharge current and on the pressure, the density ranged in various measurement runs from  $0.6 \cdot 10^{14}$  to  $2 \cdot 10^{14}$  cm<sup>-3</sup> (Ref. 20).

In the limit of low field strengths ( $\kappa \ll 1$ ) the saturated gain of the medium is given by the simple equation (Ref. 21, see also Refs. 1 and 22)

$$g \propto \operatorname{Re} w \left( \frac{\Omega + i\Gamma}{kv_{Ti}} \right) \left[ 1 - \frac{\kappa}{2} \left( 1 + \frac{\Gamma^2}{\Gamma^2 + \Omega^2} \right) \right]; \quad \Gamma = \gamma \Gamma_{mn}, \quad (3.1)$$

$$w(z) = e^{-z^2} \left( 1 + \frac{2i}{\sqrt{\pi}} \int_0^z e^{t^2} dt \right)$$

is the probability integral of complex argument. Equation (3.1) determines the implicit  $\kappa(\Omega)$  dependence, given the loss level  $g$ . The  $\kappa(\Omega)$  dependence can also be expressed explicitly by using the asymptotic form of the function  $w$ :

$$\kappa(\Omega) = 2 \frac{1 - \exp[(\Omega^2 - \Omega_i^2)/(kv_{Ti})^2]}{1 + \Gamma^2/(\Gamma^2 + \Omega^2)}, \quad (3.2)$$

where  $\Omega_i$  is the lasing shutoff frequency.

The function  $P(\Omega)$  with account taken of the frequency fluctuations under real conditions can be also represented by the convolution of  $\kappa(\Omega)$  and the laser spectrum in the single-frequency regime. The measurements have shown that the lasing spectrum can be satisfactorily approximated by a Lorentzian of width  $\Gamma_a$ . Therefore

$$P(\Omega) = \frac{A}{\pi} \int_{-\Omega_i}^{\Omega_i} \frac{\Gamma_a}{\Gamma_a^2 + (\Omega - \Omega')^2} \kappa(\Omega') d\Omega', \quad (3.3)$$

where  $A$  is a scale factor. The  $P(\Omega)$  dependence contains altogether four parameters:  $A$ ,  $\Gamma$ ,  $\Gamma_a$ , and  $\Omega_i$ . The width  $\Gamma_a$  of the instrumental function and the lasing-shutoff frequency  $\Omega_i$  were measured directly in the experiment, while the parameters  $A$  and  $\Gamma$  were used for adjustment. The theoretical curve was drawn through the experimental points with the aid of a computer, using a program based on the maximum-likelihood method. The result of the reduction of a typical Lamb-dip contour is shown in Fig. 4. The values of the dip width were obtained at different discharge parameters for the lines 4880 and 5017 Å. The statistical error of the estimate of  $\Gamma$  did not exceed 10%.

Figure 5 shows the measured values of the Lamb-dip broadening

$$\Delta\nu_c = \frac{\Gamma - \Gamma_{mn}}{\pi} = \frac{\Gamma_{mn}}{\pi} (\gamma - 1) \quad (3.4)$$

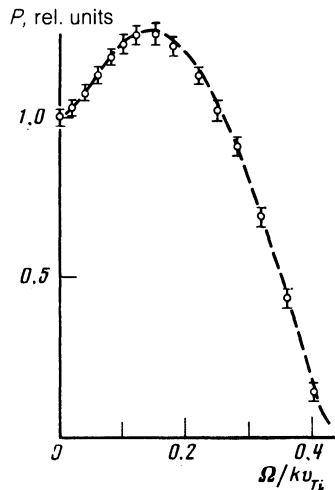


FIG. 4. Experimental values of the lasing power  $P$  vs the detuning frequency  $\Omega$ , and theoretical curve with the following parameters  $\Omega_i/kv_{Ti} = 0.405$ ;  $\Gamma_a/kv_{Ti} = 0.022$ ;  $\Gamma/kv_{Ti} = 0.082$ ;  $A = 6.55$ .

for two lines, as functions of the electron density  $n$ . All the experiments were performed with weak saturation ( $0.1 \leq \kappa \leq 0.25$ ). Each point was obtained by averaging over three or four measurements at different  $\kappa$ . The  $n_e$  measurement range was limited by the lasing range. The data for  $n_e < 1.2 \cdot 10^{14}$  were obtained by varying the discharge current in the range 100–180 A at 0.18 Torr pressure, and those for  $n_e > 1.2 \cdot 10^{14}$  cm<sup>-3</sup> were obtained by increasing the pressure and keeping the current constant 180 A. This was the maximum current used, to prevent a noticeable influence of multiply charged ions and to be able to set  $n_i = n_e$ .

The same figure shows for comparison a  $\Delta\nu_c(n_e)$  plot calculated from Eq. (2.14) without fit parameters. The value of  $\varepsilon$  was calculated from Eqs. (2.6) and (2.8), rewritten in the form

$$\varepsilon \approx 2\bar{\nu}_e/\Gamma_{mn}^2 \Gamma_{mn} \Delta\nu_D. \quad (3.5)$$

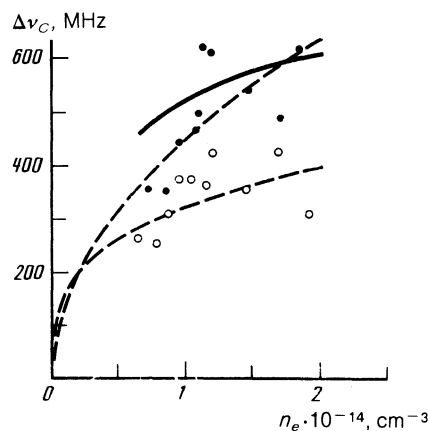


FIG. 5. Lamb-dip broadening  $\Delta\nu_c$  vs the charged-particle density  $n_e$ : ●— $\lambda = 5017$  Å, ○—4880 Å, solid line—calculated from Eq. (3.5) for the experimental conditions. Dashed—reduction of the experimental data by least squares.

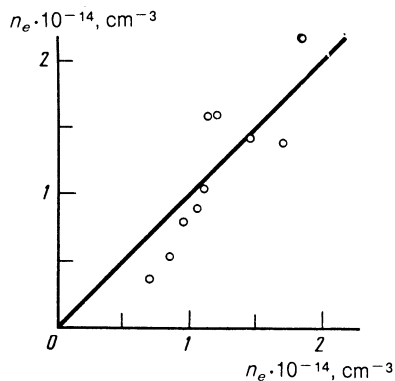


FIG. 6. Ion density  $n_i$ , determined from the broadening data, vs the electron density  $n_e$ . The straight line is drawn by the least-squares method.

Here  $\Delta\nu_D$  is the Doppler width of the line in GHz, the density  $n_e$  is in units of  $10^{14} \text{ cm}^{-3}$ , and the widths  $\Gamma_{mn}$  and  $\Gamma_m$  are in units of  $10^9 \text{ s}^{-1}$ . The homogeneous width  $\Gamma_{mn}$  and the width  $\Gamma_m$  of the upper level were substituted in (3.5), with allowance for electronic quenching.<sup>5,6</sup>

The characteristic values of the Coulomb parameters under the experimental conditions were  $\varepsilon \sim 10$ , so that the asymptotic relation  $\gamma - 1 \propto n_e^{1/2}$  could be used for (2.13). The dashed lines are plots of the functions  $\Delta\nu_C = Bn_e^\delta$ , with the parameters  $B$  and  $\delta$  obtained from the experimental points by least squares. The values  $\delta = 0.3 \pm 0.2$  and  $\delta = 0.5 \pm 0.2$  obtained respectively for the 4880 and 5017 Å lines do not contradict the hypothetical square-root dependence of the broadening on the electron density.

Figure 6 shows the density of the ions extracted from the broadening  $\Delta\nu_C$  by Eq. (3.5) as a function of  $n_e$ . It was assumed that the lifetimes of the upper levels, with allowance for quenching, are equal for both lines. The straight line  $n_i = Kn_e$  drawn by least square for the 5017 Å line has a slope  $K = 1.0 \pm 0.1$ .

#### §4. DISCUSSION

Let us discuss in greater detail the possible systematic errors in the measurement of the width  $\Gamma$ . The ion drift, with velocity  $v_D$ , was taken into account in the distribution function (2.6) with the aid of the substitution  $\mathbf{v} \rightarrow \mathbf{v} - \mathbf{v}_D$ . As shown in Ref. 14, this substitution suffices to reach an accuracy of several percent. If the gain is averaged over the wave propagation directions the value of  $P$  is decreased somewhat by the drift.<sup>23</sup> The relative change is  $\Delta P/P \sim (kv_D/\Omega_i)^2$ . The measured drift velocities did not exceed  $0.04 v_{Ti}$ , and the steady-state lasing-termination frequency was less than  $0.3k v_{Ti}$ , so that  $\Delta P/P < 0.02$ . This last estimate is confirmed by numerical calculation. A computer check of the approximation of the probability integral (3.1) by a Gaussian function has shown that the approximation error of (3.2) at the experimental parameters  $\Gamma$  and  $\kappa$  does not exceed 3%.

We estimate now the Lamb-dip broadening by mechanisms other than the Coulomb ion-ion scattering. To this end we compare the Coulomb broadening of the frequencies of elastic scattering of the ion excited states by atoms and

electrons under the experimental conditions. The atomic collisional deactivation of the laser levels ArII is apparently negligible, in view of the small cross sections  $\sigma_{CE} \approx 5 \cdot 10^{-15} \text{ cm}^2$  for resonant charge exchange<sup>24</sup> and of the cross sections  $\sigma_m \sim \sigma_{CE}$  for collisional mixing over the sublevels of the 4p configuration at  $T_e \approx 1 \text{ eV}$  (Ref. 25). The neutral-atom density in the high-current discharge of an ion laser usually does not exceed  $10^{15} \text{ cm}^{-3}$ , so that the broadening is 2 MHz.

The most important among the processes in which electrons participate are level quenching and Stark broadening. The Stark broadenings  $\Delta\nu_S = s(T_e)n_e$  of the argon ion lines, measured by various methods, are not in satisfactory agreement with one another or with Griem's calculations,<sup>2</sup> and the values of  $s$  differ by a factor 2–3. As an estimate, we choose the largest Stark coefficient of Ref. 26, viz.,  $s = 6 \cdot 10^{-13} \text{ MHz} \cdot \text{cm}^3$  ( $T_e = 2.7 \text{ eV}$ ). At the experimentally attainable electron densities the Stark broadening is then not larger than 120 MHz. The electron-deactivation constant was measured in Ref. 30 by an independent method under conditions equivalent to our experiment and amounts to  $\langle \sigma_D v \rangle \approx 4 \cdot 10^{-7} \text{ cm}^3 \cdot \text{s}^{-1}$  for the 4880 Å upper level line, in agreement with the known published data.<sup>5,6</sup> There are no experimental data on electron quenching for the lower level. We confine ourselves therefore to the approximate Born cross section from Ref. 31. The total contribution of the electron quenching at the maximum electron densities does not exceed 30 MHz. A definite contribution can be made to the measured quenching constant by inelastic ion-ion scattering. Evidence in favor of such a process is apparently offered by the Boltzmann population distribution in the sublevels within one electron configuration (see, e.g., Refs. 6 and 25) with a temperature on the order of that of the ions.

Besides collisions in a laser with a high discharge current, a definite role can be played in principle by the Zeeman splitting of the levels in the proper magnetic field of the discharge current. The splitting of the  $\sigma^+$  and  $\sigma^-$  components is  $3.5 \text{ MHz} \cdot \text{Oe}^{-1}$  for the 4880 Å line,<sup>5</sup> and the magnetic field of a 200 A current reaches 100 Oe near the walls. Recognizing that the transverse dimension  $b$  of the light beam is much smaller under our conditions than the tube radius,  $b/R \sim \frac{1}{4}$ , and assuming in the estimate that the current is uniformly distributed over the discharge cross section, we obtain a splitting  $\Delta\nu_z \lesssim 50 \text{ MHz}$ .

The assumptions made in the derivation of the equations have thus little effect on the accuracy with which  $\Gamma$  is measured. The main contribution to the possible systematic error is made apparently by the error in the determination of the instrumental width  $\Gamma_a$  and of the shutoff frequency  $\Omega_i$  (up to 25%). Inelastic collisions of the ions with atoms and electrons, and the current's magnetic self-field cannot account for the observed value of the Lamb-dip broadening.

The experimental  $\Delta\nu_C(n_e)$  plots obtained for the two lines (Fig. 5) tend to saturate at  $n_e \gtrsim 10^{14} \text{ cm}^{-3}$ . The quantitative discrepancy does not exceed the estimated systematic error and may be due to the fact that the values of  $\Gamma_a/\Gamma_{mn}$  differ substantially for these two lines. The curve calculated from (3.5) using the measured  $n_e$  and  $\Delta\nu_D$  also saturates in this parameter region. The accuracy with which the absolute value is determined is governed by the errors in the measure-

ments of  $\Delta\nu_D$  (10%),  $n_e$  (10%), and the quenching ( $\sigma_D\nu$ ) (25%). It can be stated on the basis of the foregoing analysis that the Coulomb mechanism accounts well for both the magnitude of the observed broadening and the character of the dependence on the charged-particle density.

## §5. CONCLUSION

We have shown in this paper that the Lamb dip in the frequency dependence of an argon-laser generation power is broadened by a factor of two relative to the radiative width for the 4880 Å line and by almost three times for the 5017 Å line. The absolute value of the broadening reached 400–600 MHz. A relatively accurate measurement of the broadening was made possible by the low values of the absorption parameter  $\kappa$ , whereas in the earlier studies<sup>4,14,23</sup> the collision broadening was masked by the field broadening. The agreement, within the limits of error, of the theory with the broadening and with the character of the dependence on the electron density, as well as the low values of the alternate broadening factors, attest to a Coulomb origin of the broadening.

Measurement of the Coulomb broadening can serve in principle as a basis for the diagnostics of the plasma of ion lasers. From the Lamb-dip broadening one can determine the ion density (see Fig. 6) which is quite difficult to measure by a direct method under ion-laser conditions.

The authors thank S. G. Rautian and G. I. Smirnov for a helpful discussion of the results, T. T. Timofeev for help with the experiment, and also A. V. Rodishevskii for collaboration with the computer reduction.

<sup>1</sup>S. G. Rautian, G. I. Smirnov, and A. M. Shalagin, *Nonlinear Resonances in the Spectra of Atoms and Molecules* [in Russian], Nauka, Novosibirsk, 1979.

<sup>2</sup>R. Brewer, in: *Nonlinear Spectroscopy*, N. Bloembergen, ed. North Holland, 1974, p. 87.

<sup>3</sup>G. N. Smirnov and D. A. Shapiro, *Zh. Eksp. Teor. Fiz.* **76**, 2084 (1979) [*Sov. Phys. JETP* **49**, 1054 (1979)].

<sup>4</sup>V. I. Donin, S. G. Rautian, G. I. Smirnov, and D. A. Shapiro, *Izv. AN SSSR, ser. fiz.* **45**, 1496 (1981).

<sup>5</sup>C. C. Davis and T. A. King, in: *Advances in Quantum Electronics*, Academic, 1975, Vol. 3.

<sup>6</sup>M. M. Dunn and J. N. Ross, *Progr. Quantum Electronics* **4**, 233 (1976).

<sup>7</sup>B. F. J. Luyken, *Physica (Utrecht)*, **60**, 432 (1972).

<sup>8</sup>L. D. Landau, *Collected Papers* [in Russian], Nauka, 1969, Vol. 1, p. 199 [Transl. publ. by Pergamon Press].

<sup>9</sup>S. G. Rautian, G. I. Smirnov, and D. A. Shapiro, *Dokl. Akad. Nauk SSSR* **262**, 600 (1982) [*Sov. Phys. Doklady* **27**, 75 (1982)].

<sup>10</sup>S. G. Rautian, *Zh. Eksp. Teor. Fiz.* **51**, 1176 (1966) [*Sov. Phys. JETP* **24**, 788 (1967)].

<sup>11</sup>F. F. Baryshnikov and V. S. Lisitsa, *ibid.* **82**, 1058 (1982) [**55**, 618 (1982)].

<sup>12</sup>K. Flammer, *Tables of Spheroidal Wave Functions*, [in Russian], Comp. Center, USSR Acad. Sci., 1962.

<sup>13</sup>I. V. Komarov, L. I. Ponomarev, and S. Yu. Slavyanov, *Spheroidal and Coulomb Functions* [in Russian], Nauka 1976.

<sup>14</sup>V. I. Donin, *Opt. Spektrosk.* **48**, 1065 (1980).

<sup>15</sup>A. A. Apolonskii, V. I. Donin, and T. T. Timofeev, *Kvant. Elektron. (Moscow)* **13**, 1004 (1986) [*Sov. J. Quant. Electron* **16**, 654 (1986)].

<sup>16</sup>Yu. V. Troitskii and N. D. Goldina, *Pis'ma Zh. Eksp. Teor. Fiz.* **7**, 49 (1968) [*JETP Lett.* **7**, 36 (1968)].

<sup>17</sup>G. Stephan and M. Trumper, *Phys. Rev.* **A30**, 1925 (1984).

<sup>18</sup>S. A. Babin, Preprint No. 303, Inst. Autom. and Electronics, Siberian Div., USSR Acad. Sci., Novosibirsk, 1986.

<sup>19</sup>Kh. P. Alum, Yu. A. Koval'cuk, and G. V. Ostrovskaya, *Pis'ma Zh. Tekh. Fiz.* **7**, 1359 (1981) [*Sov. Tech. Phys. Lett.* **7**, 581 (1981)].

<sup>20</sup>G. N. Alferov, S. A. Babin, and V. P. Drachev, Preprint No. 306, Inst. Autom. and Electronics, Siberian Div., USSR Acad. Sci., Novosibirsk, 1986.

<sup>21</sup>W. E. Lamb, *Phys. Rev.* **134A**, 1429 (1964).

<sup>22</sup>S. G. Rautian, *Trudy FIAN* **43**, 3 (1968).

<sup>23</sup>P. Zory, *IEEE J. Quant. Electron.* **4**, 390 (1967).

<sup>24</sup>J. B. Hasted, *Proc. Roy. Soc. (London)* **A205**, 421 (1951).

<sup>25</sup>K. Tachibana and K. Fakuda, *Mem. Fac. Eng. Kyoto Univ.* **35**, 79 (1973).

<sup>26</sup>D. E. Roberts, *J. Phys.* **B1**, 53 (1968).

<sup>27</sup>P. H. M. Vaessen, J. M. L. van Engelen, and J. J. Bleize, *JQSRT* **33**, 51 (1985).

<sup>28</sup>V. V. Lebedeva, A. I. Odintsov, N. A. Glavatskikh, L. E. Grin', and A. G. Shul'ga, *Zh. Prikl. Spektrosk.* **41**, 385 (1984).

<sup>29</sup>H. R. Griem, *Spectral Line Broadening by Plasmas*, Academic, 1974.

<sup>30</sup>A. A. Apolonskii, S. A. Babin, and T. T. Timofeev, *Opt. Spektrosk.* **59**, 714 (1985).

<sup>31</sup>L. A. Vaïnshtein, I. I. Sobel'man, and E. A. Yukov, *Excitation of Atoms and Broadening of Spectral Lines* [in Russian], Nauka, 1979.

Translated by J. G. Adashko